Journal of ELECTRONIC MATERIALS, Vol. 47, No. 12, 2018
https://doi.org/10.1007/s11664-018-6632-8

High Rate Growth of MOCVD-Derived GdYBCO Films Based on a Simple Self-Heating Method

RUIPENG ZHAO,[1] QING LIU,[1] FEI ZHANG,[2] YUDONG XIA,[3] HAO TANG,[1] YUMING LU,[4] CHUANBING CAI,[4] BOWAN TAO,[1,5] and YANRONG LI[1]

1.—State Key Lab of Electronic Thin Films and Integrated Devices, University of Electronic Science and Technology of China, Chengdu 610054, People's Republic of China. 2.—Chengdu Fine Optical Engineering Research Center, Chengdu 610041, People's Republic of China. 3.—School of Physical Science and Technology, Southwest Jiaotong University, Chengdu 610031, People's Republic of China. 4.—School of Physics, Shanghai University, Shanghai 200444, People's Republic of China. 5.—e-mail: taobw@uestc.edu.cn

The home-designed metal organic chemical vapor deposition (MOCVD) system was applied to prepare the $Gd_{0.5}Y_{0.5}Ba_2Cu_3O_{7-\delta}$ (GdYBCO) films at a high deposition rate in order to improve the production efficiency and reduce the preparation cost of high temperature superconducting tapes. Based on a simple self-heating method, the distance between the shower head and the substrate surface can be reduced effectively to increase the concentration of metal organic sources on the substrate surface, which can commendably improve the deposition rate of GdYBCO films and the utilization ratio of metal organic sources. At last, the GdYBCO films were successfully prepared on the $LaMnO_3$ template at the high deposition rate of 1 μm/min by the MOCVD process based on the simple self-heating method and the critical current (I_c) was more than 220 A/cm-width (77 K, 0 T), corresponding to the critical current density (J_c) more than 4.4 MA/cm^2 (77 K, 0 T).

Key words: High deposition rate, GdYBCO, MOCVD, self-heating, critical current density

INTRODUCTION

$REBa_2Cu_3O_{7-\delta}$ [(REBCO), RE = rare earth elements] high temperature superconducting (HTS) tapes, which are also called coated conductors, are comprehensively studied by many research groups for their applications in the electric power field.[1–3] Because of its high current capacity and large irreversible field, REBCO HTS tapes have significant potential for application in the aspects of superconducting cables, strong magnets, superconducting motors, generators and superconducting current limiters.[4–6] However, the large-scale applications of REBCO HTS tapes need not only the high critical current, but also the high fabrication rate, which can directly affect the preparation efficiency. Therefore, many research teams around the world are working to improve performance and preparation efficiency, which meet the increasing demands of application products on the superconducting tapes.[7–10] At present, the main process methods, which are adopted to prepare REBCO superconducting films, are metal organic deposition (MOD), pulsed laser deposition (PLD), reactive co-evaporation (RCE) and metal organic chemical vapor deposition (MOCVD).[11–15] The MOCVD process method used for the preparation of the GdYBCO films in the present research has several advantages, such as low requirements for vacuum equipment and large area uniform preparation of superconducting films, which is considered to be a feasible process method to improve preparation efficiency. Although many studies about the high rate growth of REBCO films have been reported, they declare the difficulty of improving the performance and the growth rate at the same time.[16]

(Received October 10, 2017; accepted August 28, 2018; published online September 28, 2018)

According to the growth thermodynamics of REBCO film, the c-axis-oriented grain is considered to be more stable than a-axis-oriented grain. However, with the increase of deposition rate of REBCO film, the growth of a-axis-oriented grains occupies the relative advantage according to the growth kinetics of REBCO film.[16,17] Therefore, the preferential growth of the REBCO film lies in the competition between the c-axis-oriented growth and the a-axis-oriented growth through the control of the process conditions. On the premise of ensuring the preferential growth of grains and good performance, the high rate growth of REBCO films attracted the attention of researchers. Nowadays, many research groups have focused on the rapid growth of REBCO films through employing various technologies.[18] Ibi et al. reported that the $EuBa_2Cu_3O_{7-\delta}$ (EuBCO) with $BaHfO_3$ coated conductors were fabricated by the PLD method at the high deposition rate of about 40 μm/h.[19] Nakaoka et al. reported that the $YBa_2Cu_3O_{7-\delta}$ (YBCO) coated conductors with high critical current were obtained using the MOD process at the thickness per single coating of 0.49 μm/coat.[20,21] Matias et al. demonstrated that the YBCO coated conductors were prepared on ion-beam-assisted-deposition- (IBAD-) textured templates by reactive co-evaporation at the deposition rate of 0.36 μm/min.[22,23] Selvamanickam et al. reported the reel-to-reel fabrication of YBCO films with the high deposition rate of 0.72 μm/min through adopting the normal chemical vapor deposition (CVD) process.[24] Miyata et al. reported the high deposition rates of 58 μm/h of high-J_c YBCO films with more than 1.8 MA/cm^2, which were prepared by using an IR-laser-assisted chemical vapor deposition (IRL-CVD) technique.[25] The studies about the deposition rate of the REBCO films are to improve the preparation efficiency of the superconducting tapes.

In our study, the $Gd_{0.5}Y_{0.5}Ba_2Cu_3O_{7-\delta}$ (GdYBCO) films were prepared at the high growth rate of 1 μm/min through using a self-heating technology.[26–28] Figure 1 shows that the simple self-heating technology is applied in our home-made MOCVD system, and the current is introduced to the metal tapes through the designed brushes. The heat generated by the Joule effect, which can meet the growth demand of GdYBCO superconducting film, is conducted from the metal tape to the buffer surface. Compared with the common heating-wire radiation heating method, the self-heating method can avoid the problem that the temperature of the shower is too high when the shower head is very close to the surface of template tape. The distance between the shower head and the metal tape can be reduced through using the self-heating method and the deposition rate of GdYBCO films can be greatly improved. Moreover, the preparation and research of the buffer template of REBCO superconducting tape is mainly based on the ion beam assisted deposition (IBAD) technology and rolling assisted biaxially textured substrates (RABiTS) technology.

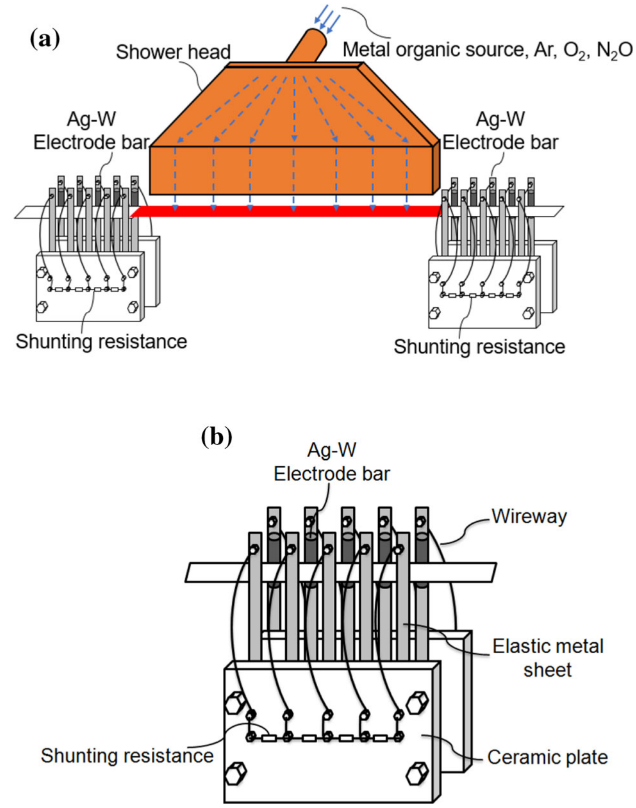

Fig. 1. (a) Schematic diagram of GdYBCO film preparation. (b) Schematic diagram of the heating electrode.

Compared to RABiTS, the IBAD process has the advantage in the cost and product performance.[29–32] In our experiments, the templates of $LaMnO_3$/epitaxial MgO/IBAD-MgO/solution deposition planarization (SDP)-Y_2O_3/Hastelloy tape were adopted to prepare GdYBCO films, as is shown in Fig. 2. Therefore, in this study, the high rate growth of high quality GdYBCO films with high critical current density (J_c) based on the self-heating technology has been intensively investigated.

EXPERIMENTAL

In our experiments, the precursors of metal organic sources were prepared by dissolving the metal organic sources of $Gd(tmhd)_3$, $Y(tmhd)_3$, $Ba(tmhd)_2$·(1,10-phenanthroline)$_2$ and $Cu(tmhd)_2$ (tmhd: 2,2,6,6-tetramethyl-3,5-heptanedionate) in tetrahydrofuran (THF). Firstly, the prepared precursors were quickly atomized by a home-made nozzle and evaporated rapidly by the heating evaporator in the MOCVD system. Then, the vapors of metal organic sources, which were mixed with the argon, oxygen and nitrous oxide, were transported into the reaction chamber and reacted to grow GdYBCO films on the surface of the templates of $LaMnO_3$/epitaxial MgO/IBAD-MgO/solution deposition planarization (SDP)-Y_2O_3/Hastelloy tape. Lastly, the GdYBCO superconducting tapes were annealed in flowing oxygen at 500°C, and the furnace was naturally cooled to room temperature with the stable oxygen flow. The distance between the shower head and the substrate is 10 mm, and the growth rate of GdYBCO films was adjusted by modulating the pumping speed of the single precursor solution. The 500 nm thick GdYBCO films were prepared at the growth rate of 300 nm/min and 1 μm/min by adjusting the precursor delivery speed of 0.8 mL/min and 2.5 mL/min and using the oxygen flow of 0.48 L/min and 1.44 L/min, respectively. Meanwhile, the process conditions of GdYBCO films at the high deposition rate of 1 μm/min, such as the heating current and the ratio of metal organic sources, were investigated in detail. The concentrations of $Zr(tmhd)_4$, $Gd(tmhd)_3$, $Y(tmhd)_3$, $Ba(tmhd)_2$·(1,10-phenanthroline)$_2$, and $Cu(tmhd)_2$ in the liquid phase precursor were 0.0045, 0.045, 0.045, 0.15, and 0.165 mol L^{-1}, respectively. The heating current (I_h) of 27.0 A and Cu/Ba ratio (r_s) of 1.1 are applied to prepare the GdYBCO film at the growth rate of 300 nm/min. For the preparation process with the growth rate of 1 μm/min, the I_h was changed from 27.0 A to 27.6 A, and the r_s was transformed from 1.1 to 1.0, respectively.

X-ray diffraction (XRD) patterns were measured using Cu K_α radiation (λ = 1.5406 Å) in the mode of θ–2θ step-scan, ω-scan, φ-scan and *Chi*-scan for the samples by an XRD system (XRD, Bede D1 system). The root-mean-square (RMS) roughness of the LaMnO$_3$ (LMO) template layer was characterized by an atomic force microscope (AFM, Seiko SPA300HV). The images of surface morphology were characterized by a scanning electron microscope (SEM, JEOL7500F). And the composition of thin films was characterized by an energy dispersive spectrometer (EDS, Oxford INCA). The

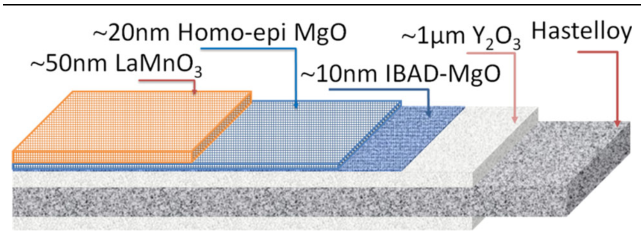

Fig. 2. The configuration diagram of the layer stack indicating thicknesses of buffer layers on the Hastelloy tape.

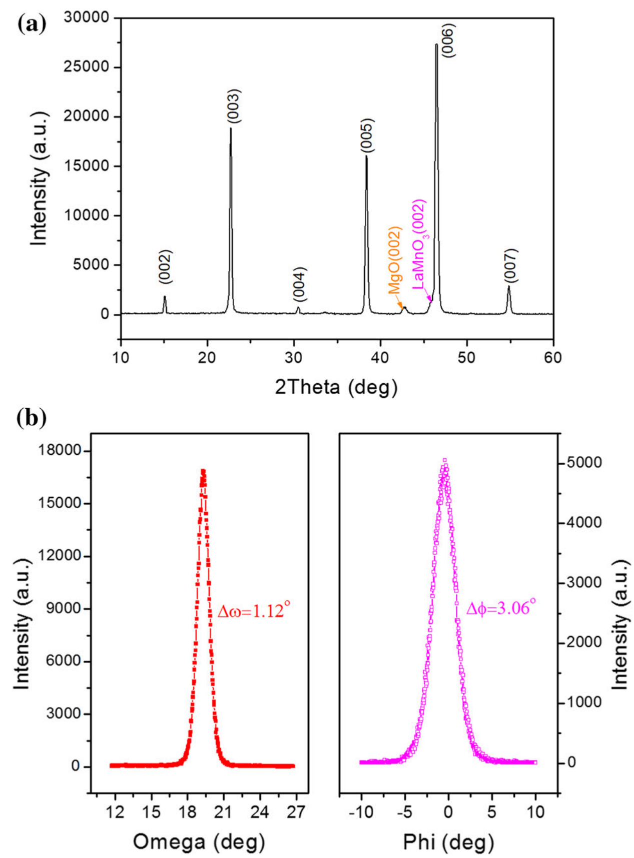

Fig. 4. (a) XRD θ–2θ scan patterns of GdYBCO film prepared at the deposition rate of 300 nm/min; (b) XRD ω-scan pattern of GdYBCO (005) and φ-scan pattern of GdYBCO (103).

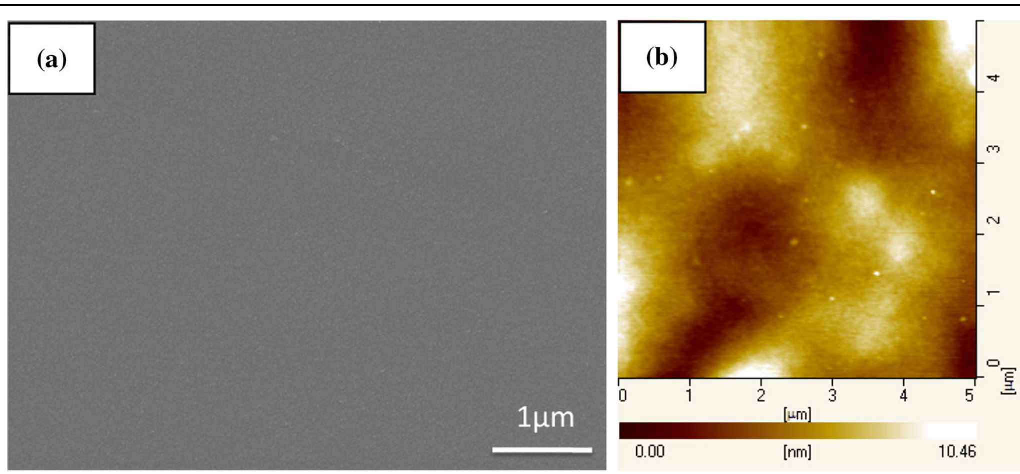

Fig. 3. (a) SEM image of the LaMnO$_3$ template and (b) AFM image of the LaMnO$_3$ template, R_{rms}= 1.75 nm.

thickness was measured by a step profiler (Veeco Dektak 150). Moreover, the J_c and critical current (I_c) at 77 K and 0 T were obtained by the Leipzig J_c-scan system and four-probe-method measurement system.

RESULTS AND DISCUSSION

The Preparation of GdYBCO Films at the Growth Rate of 300 nm/min

The used LMO template surface was characterized by the AFM and SEM, as are shown in Fig. 3. Figure 3a is the SEM test result of $LaMnO_3$ film morphology, and its surface is very dense and smooth. And the AFM test result of Fig. 3b shows that its RMS roughness over an area of $5 \times 5\ \mu m^2$ is 1.75 nm. Therefore, the LMO template can completely meet the demand of epitaxial growth of highly biaxially textured GdYBCO films on the flat surface.

Based on the smooth LMO template, the preparation process conditions of GdYBCO films can be optimized at the relatively low precursor delivery speed of 0.8 mL/min. By employing the appropriate process conditions, such as I_h and metal organic sources ratio, 500 nm thick GdYBCO films were prepared on the LMO template at the growth rate of 300 nm/min. The XRD θ–2θ step-scan measurement has been performed on the deposited GdYBCO superconducting film, and the result is shown in Fig. 4a. As is shown in Fig. 4a, the clear GdYBCO (*00l*) peaks are observed in the curve of the sample prepared at an I_h of 27.0 A and a r_s of 1.1 and the intensity of the GdYBCO (*00l*) peaks is relatively strong, which indicates the formation of *c*-axis-oriented GdYBCO grains in the crystallized film. In addition to the diffraction peaks of biaxially textured GdYBCO superconducting films, the MgO (002) and $LaMnO_3$ (002) peaks of the LMO template are also observed in the curve of a θ–2θ pattern. Therefore, there are only the GdYBCO (*00l*) peaks without basically any other impurity diffraction peaks, which shows that the process conditions are appropriate at the deposition rate of 300 nm/min. What is more, the XRD ω-scan of GdYBCO (005) and the XRD φ-scan of GdYBCO (103) have also been performed, which were used to characterize out-of-plane and in-plane textures. Figure 4b shows the measured curves of the ω-scan and the φ-scan and the corresponding full width at half maximum (FWHM) values are 1.12° and 3.06°, respectively. The biaxial texture of the prepared GdYBCO film is very good.

The SEM image of the surface morphology of the GdYBCO superconducting film prepared at an I_h of 27.0 A and a r_s of 1.1 is obtained by a SEM system. Figure 5 shows the morphology image of the sample prepared at the growth rate of 300 nm/min. The surface of GdYBCO film is very flat and the impurity precipitates did not appear. Therefore, the surface morphology is in accord with the characterization results of XRD. Meanwhile, the J_c at 77 K and 0 T are measured and can reach 4.4 MA/cm^2. Therefore, the I_h of 27.0 A and r_s of 1.1 are considered to be the appropriate process parameters based on the deposition rate of 300 nm/min. However, the deposition rate of 300 nm/min will still influence the improvement of preparation efficiency. So the higher rate growth of GdYBCO films needs to be studied well.

The Preparation of GdYBCO Films at the Growth Rate of 1 μm/min

Because of the use of the self-heating method, the shower head can be very close to the surface of metal tapes. In order to study the rapid deposition of superconducting films, 500 nm thick GdYBCO films

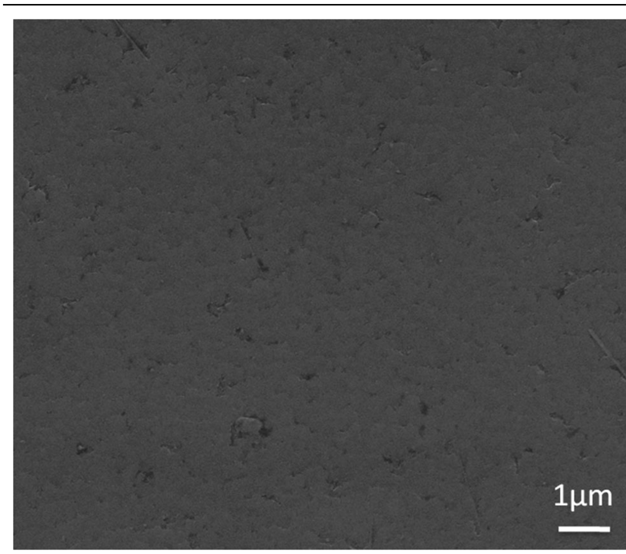

Fig. 5. SEM image of GdYBCO film prepared at the deposition rate of 300 nm/min.

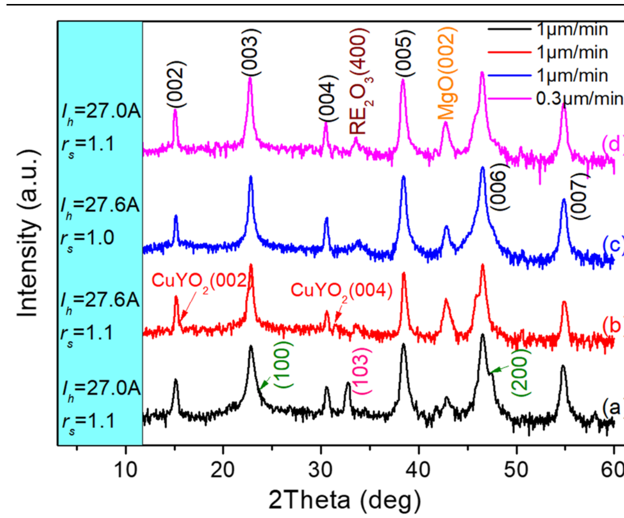

Fig. 6. XRD θ–2θ scan patterns of GdYBCO films prepared at the deposition rate of 1 μm/min and 0.3 μm/min.

were also deposited on the same LMO template at the high growth rate of 1 μm/min. Thus, increasing the injection rate of the precursor solution can greatly increase the deposition rate of GdYBCO films. So the delivery rate of precursor is increased from 0.8 mL/min to 2.5 mL/min and the deposition rate is also increased from 0.3 μm/min to 1 μm/min. Meanwhile, the process parameters including I_h and r_s were adjusted to prepare GdYBCO films with good structure and performance.

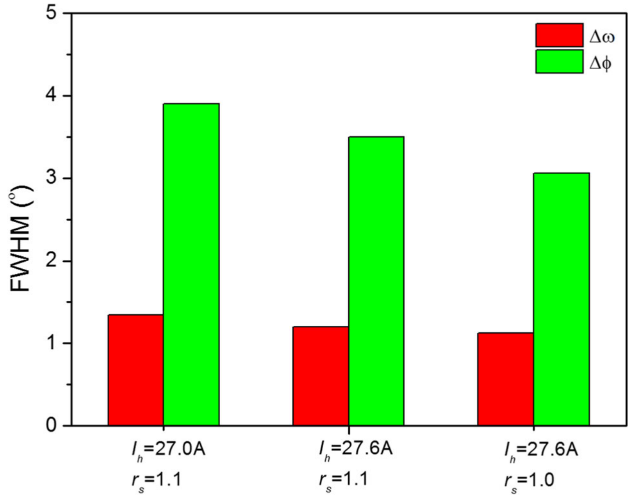

Fig. 7. Variations in the FWHM values of XRD ω-scans and φ-scans with I_h and r_s at the deposition rate of 1 μm/min.

The XRD θ–2θ scan patterns of GdYBCO films prepared at the different I_h and r_s values are performed by an XRD system, as shown in Fig. 6. At the I_h of 27.0 A and r_s of 1.1, there are the obvious GdYBCO (100) and (200) peaks in the θ–2θ curve, which indicates that the heating temperature cannot satisfy the demand of the pure c-axis-oriented grains growth of GdYBCO superconducting films. For the growth of REBCO films, the insufficient heating temperature will cause the REBCO grains to grow along the a-axis direction. Moreover, there is the GdYBCO (103) diffraction peak, which shows that the tilted grains are formed in the superconducting film. Then the Cu-O planes of the a-axis-oriented grains and (103) oriented grains will deviate from the Cu-O planes of other c-axis-oriented grains, which will greatly affect the conduction of superconducting current. Therefore, the appropriate process conditions at the growth rate

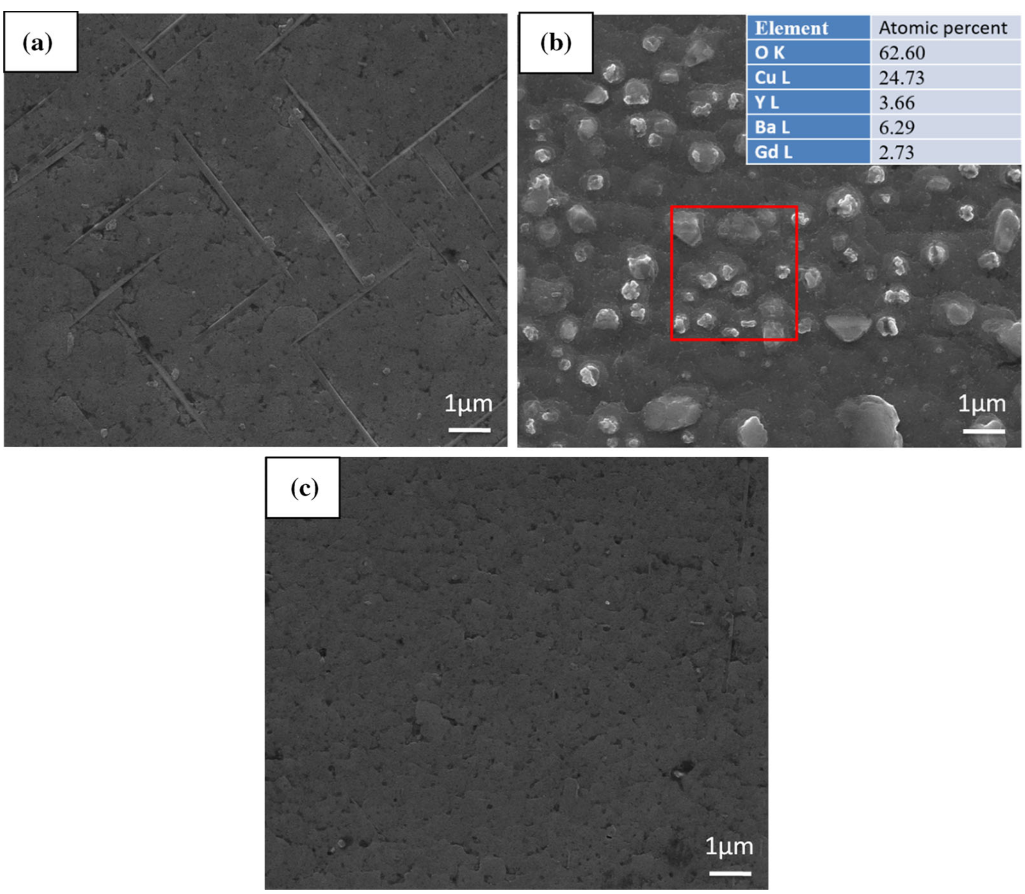

Fig. 8. SEM images of GdYBCO films prepared at the deposition rate of 1 μm/min: (a) I_h= 27.0 A, r_s= 1.1; (b) I_h= 27.6 A, r_s= 1.1; (c) I_h= 27.6 A, r_s= 1.0.

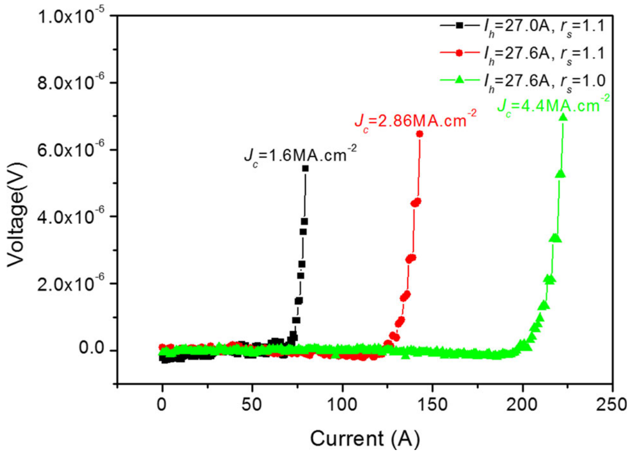

Fig. 9. Variation in the I_c values GdYBCO films with I_h and r_s at the deposition rate of 1 μm/min.

of 1 μm/min are different from the parameters at the growth rate of 0.3 μm/min. With the increasing of I_h from 27.0 A to 27.6 A, the peaks of GdYBCO (100), (200) and (103) are basically eliminated. There are only the GdYBCO (*00l*) peaks in the θ–2θ curve, which indicates that the GdYBCO grains are *c*-axis-oriented in the film. However, the diffraction peaks of the $CuYO_2$ impurity appear in the XRD θ–2θ scan curve, indicating that the r_s deviates from the optimum parameter with the increase of heating temperature of superconducting tape. Therefore, with the decreasing of r_s from 1.1 to 1.0, the diffraction peaks of the $CuYO_2$ phase disappear at the I_h of 27.6 A and the GdYBCO (*00l*) peaks are also enhanced due to the suitable process conditions. And the test result at the deposition rate of 1 μm/min is similar to that of at the deposition rate of 0.3 μm/min, as shown in Fig. 6. The excessive heating temperature can cause the decomposition of REBCO films and the production of impurities.

Similarly, every full width at half maximum (FWHM) value by fitting every curve of the XRD GdYBCO (005) ω-scan and GdYBCO (103) φ-scan is listed according to the different I_h and r_s. The XRD ω-scan of GdYBCO (005) and φ-scan of GdYBCO (103) were performed, which were used to characterize out-of-plane and in-plane textures. The corresponding FWHM values of the ω-scan and φ-scan curves are shown in Fig. 7. At the I_h of 27.6 A and the r_s of 1.0, the FWHM values of the ω-scan and φ-scan curves are individually 1.1° and 3°, which are the smallest among the different process conditions of I_h and r_s. Meanwhile, the FWHM values of the deposited GdYBCO film at the growth rate of 1 μm/min can reach that of the GdYBCO film at the growth rate of 0.3 μm/min, which shows its good biaxial texture.

The surface morphologies of the superconducting films are observed by a SEM system. Figure 8 shows the morphological images of these prepared samples at the growth rate of 1 μm/min. At the I_h of 27.0 A and the r_s of 1.1, the *a*-axis-oriented grains can be identified as rod-like objects in the image, as is shown in Fig. 8a. As the I_h is raised from 27.0 A to 27.6 A, the *a*-axis-oriented GdYBCO grains disappeared, and the irregularly shaped outgrowths are formed on the surface of the film, as shown in Fig. 8b. The EDS revealed that the impurities are poor barium outgrowths. At the I_h of 27.6 A and the r_s of 1.0, the surface of the prepared GdYBCO film is very flat and dense. The surface morphologies are in accord with the characterization results of XRD.

For these samples prepared at the different I_h and r_s, the I_c at 77 K and 0 T are measured by the induction and four-probe methods, and the corresponding measured results are shown in Fig. 9. The I_c of the sample prepared at the I_h of 27.0 A and r_s of 1.1 is only 80 A/cm-width, corresponding to the J_c reaching 1.6 MA/cm^2 (77 K, 0 T). With the increasing of I_h from 27.0 A to 27.6 A, its I_c rises to 143 A/cm-width, corresponding to the J_c more than 2.8 MA/cm^2 (77 K, 0 T). As the r_s drops from 1.1 to 1.0, the I_c of the sample prepared at the I_h of 27.6 A rises from 140 A/cm-width to 220 A/cm-width, corresponding to the J_c more than 4.4 MA/cm^2 (77 K, 0 T). The performance of GdYBCO films prepared at the high growth rate of 1 μm/min can reach that of GdYBCO films prepared at the high growth rate of 0.3 μm/min.

CONCLUSION

In this study, a self-heating method is used to prepare GdYBCO films by us. Different from the conventional radiation heating method, the shower head can be very close to the metal tapes without excessive temperature. Therefore, the deposition rate of GdYBCO films can be greatly increased from 0.3 μm/min to 1 μm/min. What is more, the J_c can be improved to reach 4.4 MA/cm^2 (77 K, 0 T) through adjusting the process conditions. Thus, it is concluded that the GdYBCO film with high J_c at the high deposition rate of 1 μm/min could be successfully prepared.

ACKNOWLEDGEMENTS

This work is supported by the National High-tech R&D Program (No. 2014AA032702). Meanwhile, we also acknowledge the support of the National Natural Science Foundation of China (No. 51702265).

REFERENCES

1. M.W. Rupich, X.P. Li, S. Sathyamurthy, C.L.H. Thieme, K. DeMoranville, J. Gannon, and S. Fleshler, *IEEE Trans. Appl. Supercond.* 23, 6601205 (2013).
2. Y.F. Zhang, T.F. Lehner, T. Fukushima, H. Sakamoto, and D.W. Hazelton, *IEEE Trans. Appl. Supercond.* 24, 7500405 (2014).
3. V. Selvamanickam, Y. Chen, X. Xiong, Y. Xie, X. Zhang, A. Rar, M. Martchevskii, R. Schmidt, K. Lenseth, and J. Herrin, *Phys. C* 468, 1504 (2008).

4. H.J. Sung, M. Park, B.S. Go, and I.K. Yu, *Supercond. Sci. Technol.* 29, 054001 (2016).
5. X.Y. Chen, J.X. Jin, Y. Xin, B. Shu, C.L. Tang, Y.P. Zhu, and R.M. Sun, *IEEE Trans. Appl. Supercond.* 24, 3801606 (2014).
6. Y.B. Zheng, Y.S. Wang, W. Pi, P. Ju, and Y.S. Wang, *Phys. C* 507, 59 (2014).
7. P. Zhao, A. Ito, R. Tu, and T. Goto, *Supercond. Sci. Technol.* 23, 125010 (2010).
8. M. Dürrschnabel, Z. Aabdin, M. Bauer, R. Semerad, W. Prusseit, and O. Eibl, *Supercond. Sci. Technol.* 25, 105007 (2012).
9. H.S. Kim, S.S. Oh, H.S. Ha, D. Youm, S.H. Moon, J.H. Kim, S.X. Dou, Y.U. Heo, S.H. Wee, and A. Goyal, *Sci. Rep.* 4, 04744 (2014).
10. R.P. Zhao, F. Zhang, Q. Liu, Y.D. Xia, Y.M. Lu, C.B. Cai, B.W. Tao, and Y.R. Li, *Supercond. Sci. Technol.* 29, 065015 (2016).
11. K. Nakaoka, M. Yoshizumi, Y. Usui, T. Izumi, and Y. Shiohara, *Phys. Proced.* 58, 134 (2014).
12. H. Yamada, H. Yamasaki, K. Develos-Bagarinao, Y. Nakagawa, Y. Mawatari, J.C. Nie, H. Obara, and S. Kosaka, *Supercond. Sci. Technol.* 17, 58 (2004).
13. V. Matias, E.J. Rowley, Y. Coulter, B. Maiorov, T. Holesinger, C. Yung, V. Glyantsev, and B. Moeckly, *Supercond. Sci. Technol.* 23, 014018 (2010).
14. T. Aytug, M. Paranthaman, E.D. Specht, Y. Zhang, K. Kim, Y.L. Zuev, C. Cantoni, A. Goyal, D.K. Christen, V.A. Maroni, Y. Chen, and V. Selvamanickam, *Supercond. Sci. Technol.* 23, 014005 (2010).
15. V. Selvamanickam, M.H. Gharahcheshmeh, A. Xu, Y. Zhang, and E. Galstyan, *Supercond. Sci. Technol.* 28, 072002 (2015).
16. H. Izumi, K. Ohata, T. Sawada, T. Morishita, and S. Tanaka, *Jpn. J. Appl. Phys.* 30, 1956 (1991).
17. F. Zhang, J. Xiong, R.P. Zhao, Y. Xue, H. Wang, Q.L. Wang, Y.Y. He, P. Zhang, and B.W. Tao, *J. Supercond. Nov. Magn.* 28, 2697 (2015).
18. P. Zhao, A. Ito, T. Kato, D. Yokoe, T. Hirayama, and T. Goto, *Supercond. Sci. Technol.* 26, 055020 (2013).
19. A. Ibi, T. Yoshida, T. Izumi, Y. Shiohara, D. Yokoe, T. Kato, and T. Hirayama, *Phys. Procedia* 81, 97 (2016).
20. K. Nakaoka, M. Yoshizumi, Y. Usui, T. Izumi, and Y. Shiohara, *Phys. Procedia* 58, 134 (2014).
21. K. Nakaoka, M. Yoshizumi, Y. Usui, T. Izumi, and Y. Shiohara, *Phys. Procedia* 27, 196 (2012).
22. V. Matias, E.J. Rowley, Y. Coulter, B. Maiorov, T. Holesinger, C. Yung, V. Glyantsev, and B. Moeckly, *Supercond. Sci. Technol.* 23, 014018 (2010).
23. V. Matias and R.H. Hammond, *Phys. Procedia* 36, 1440 (2012).
24. V. Selvamanickam, Y. Xie, J. Reeves, and Y. Chen, *MRS Bull.* 29, 579 (2004).
25. S. Miyata, K. Matsuse, A. Ibi, T. Izumi, Y. Shiohara, and T. Goto, *Supercond. Sci. Technol.* 26, 045020 (2013).
26. F. Zhang, R.P. Zhao, Y. Xue, H. Wang, Y.Y. He, P. Zhang, B.W. Tao, J. Xiong, and Y.R. Li, *Appl. Phys. A* 122, 81 (2016).
27. R.P. Zhao, F. Zhang, Q. Liu, Y.D. Xia, Y.M. Lu, C.B. Cai, J. Xiong, B.W. Tao, and Y.R. Li, *Supercond. Sci. Technol.* 30, 025023 (2017).
28. H.Y. Zhai, H.M. Christen, P.M. Martin, L. Zhang, and D.H. Lowndes, *IEEE Trans. Appl. Supercond.* 13, 2622 (2003).
29. C. Sheehan, Y. Jung, T. Holesinger, D.M. Feldmann, C. Edney, J.F. Ihlefeld, P.G. Clem, and V. Matias, *Appl. Phys. Lett.* 98, 071907 (2011).
30. M.P. Paranthaman, T. Aytug, L. Stan, Q. Jia, C. Cantoni, and S.H. Wee, *Supercond. Sci. Technol.* 27, 022002 (2014).
31. Y. Xue, Y.H. Zhang, F. Zhang, R.P. Zhao, H. Wang, J. Xiong, and B.W. Tao, *J. Alloy. Compd.* 673, 47 (2016).
32. S. Kreiskott, P.N. Arendt, J.Y. Coulter, P.C. Dowden, S.R. Foltyn, B.J. Gibbons, V. Matias, and C.J. Sheehan, *Supercond. Sci. Technol.* 17, S132 (2004).